Dual Role of the 1,2,3-Triazolium Ring as a Hydrogen-Bond Donor and Anion–π Receptor in Anion-Recognition Processes

ARTICLE *in* CHEMISTRY - A EUROPEAN JOURNAL · JUNE 2015

Impact Factor: 5.73 · DOI: 10.1002/chem.201500231

6 AUTHORS, INCLUDING:

Antonio Caballero
University of Murcia
51 PUBLICATIONS **1,796** CITATIONS
SEE PROFILE

Ibon Alkorta
Spanish National Research Council
680 PUBLICATIONS **12,435** CITATIONS
SEE PROFILE

José Elguero
Spanish National Research Council
1,502 PUBLICATIONS **22,232** CITATIONS
SEE PROFILE

Pedro Molina
University of Murcia
503 PUBLICATIONS **7,790** CITATIONS
SEE PROFILE

ChemPubSoc Europe

DOI: 10.1002/chem.201500231

CHEMISTRY
A European Journal
Full Paper

Anion Recognition

Dual Role of the 1,2,3-Triazolium Ring as a Hydrogen-Bond Donor and Anion–π Receptor in Anion-Recognition Processes

Fabiola Zapata,[a] Lidia Gonzalez,[a] Antonio Caballero,*[a] Ibón Alkorta,*[b] Jose Elguero,[b] and Pedro Molina*[a]

Abstract: Several bis(triazolium)-based receptors have been synthesized as chemosensors for anion recognition. The central naphthalene core features two aryltriazolium side-arms. NMR experiments revealed differences between the binding modes of the two triazolium rings: one triazolium ring acts as a hydrogen-bond donor, the other as an anion–π receptor. Receptors $\mathbf{9}^{2+}\cdot\mathbf{2BF_4}^-$ (C_6H_5), $\mathbf{11}^{2+}\cdot\mathbf{2BF_4}^-$ (4-NO_2–C_6H_4), and $\mathbf{13}^{2+}\cdot\mathbf{2BF}^{4-}$ (ferrocenyl) bind $HP_2O_7^{3-}$ anions in a mixed-binding mode that features a combination of hydrogen-bonding and anion–π interactions and results in strong binding. On the other hand, receptor $\mathbf{10}^{2+}\cdot\mathbf{2\,BF_4}^-$ (4-CH_3O–C_6H_4) only displays combined Csp_2–H/anion–π interactions between the two arms of the receptors and the bound anion rather than triazolium $(CH)^+\cdots$anion hydrogen bonding. All receptors undergo a downfield shift of the triazolium protons, as well as the inner naphthalene protons, in the presence of $H_2PO_4^-$ anions. That suggests that only hydrogen-bonding interactions exist between the binding site and the bound anion, and involve a combination of cationic (triazolium) and neutral (naphthalene) C–H donor interactions. Theoretical calculations relate the electronic structure of the substituent on the aromatic group with the interaction energies and provide a minimum-energy conformation for all the complexes that explains their measured properties.

Introduction

Among the most promising anion-binding strategies that have recently attracted much attention in the literature are those involving hydrogen bonding between a C–H donor unit and an anion and the so-called anion–π interactions.[1] The nitrogen-rich 1,2,3-triazole ring features highly polarized carbon atoms, which allow the complexation of anions by hydrogen bonding,[2] Two sources that contribute to the unexpected anion-binding affinity of the 1,2,3-triazole unit have been reported.[3] First, the electronegativities of the three nitrogen atoms combine to polarize the C–H bond. Second, the electron lone pairs on the nitrogen atoms act to establish and orient a large 5D dipole along the C–H bond, with its positive end directed almost in line with the C(5)–H bond. These combined effects allow the complexation of anions by (charge-assisted) hydrogen bonds, with hydrogen-bond-donor strengths approaching those of amides and imidazolium rings.[4–7]

In addition, coordination or protonation of heteroaromatic rings has a strong influence on the anion-binding capability of the receptor, and significantly increases their π acidity, which consequently enhances the ability of the ring to interact favorably with anions.[8] The binding ability of C(5)–H···A^- (A = Anion) is strongly enhanced by converting the 1,2,3-triazole unit into a 1,2,3-triazolium cation; the latter is expected to be an even-more-efficient anion captor, and uses anion–π interactions as an alternative binding mechanism.[9,10] It is well known that anion–π interactions participate in the formation of robust recognition motifs and it was expected that these complexes would exhibit very large binding energies due to the strong electrostatic effects that dominate the interaction.[11]

The chelating ability of 1,2,3-triazolium ligands to dianions can be easily tuned by transforming the ligands into tridentate structures or creating multivalent macrocycles.[12] It has been demonstrated that this kind of receptor strongly complexes oxoanions, whereas the nonmethylated analogues show very weak interactions under similar conditions.[13,14] Ultimately, by clicking two building blocks into place, the 1,2,3-triazole ring emerges as a versatile functional unit, which permits very successful application. In this context, the preparation via click chemistry renders the 1,2,3-triazole ring particularly suited to the construction of restricted architectures, such as macrocyclic anion receptors. For example, a tetra-1,2,3-triazolium macrocycle[15] and tetra-1,2,3-triazolium cage[16] have demonstrated that these highly charged receptors exhibit strong anion-binding affinities, involving hydrogen bonds in all cases, towards oxoanions.

Typically, anion–π interactions are favorable noncovalent contacts between an electron-deficient (π acidic) aromatic

[a] Dr. F. Zapata, L. Gonzalez, Dr. A. Caballero, Prof. P. Molina
Departamento de Química Orgánica, Universidad de Murcia
Campus de Espinardo, 30100, Murcia (Spain)
E-mail: antocaba@um.es
pmolina@um.es

[b] Prof. I. Alkorta, Prof. J. Elguero
Instituto de Química Médica
Consejo Superior de Investigaciones Científicas (CSIC)
Juan de la Cierva, 3, 28006, Madrid (Spain)
E-mail: ibon@iqm.csic.es

Supporting information for this article is available on the WWW under http://dx.doi.org/10.1002/chem.201500231.

system and an anion.[17] This interaction is proposed to arise from a negatively charged species with a Coulombic attraction to an area of low electron density in an electron-deficient aromatic ring. Despite the numerous solid-state examples, theoretical treatments,[18] significant interest in the fundamental nature of the interaction, and its potential application, surprisingly few solution-phase examples recognize the anion–π interaction.[19,20]

Recently, it has been reported that the *cis* isomer of a hexapyrrolic calix[4]pyrrole binds anions in a mixed-binding mode by a combination of hydrogen bonding and anion–π interactions, whereas the *trans* isomer displays only hydrogen-bonding interactions.[21] In this context, we are interested in pursuing this goal to create receptors in which selectivity does not arise from size- and shape matching with a particular anionic guest, but rather from the combined intrinsic anion preference of two distinct noncovalent interactions.[22–24] Herein, we describe a receptor capable of anion binding by a combination of both hydrogen-bonding and anion–π interactions with a 1,2,3-triazolium binding site, in which one ring acts as a hydrogen-bond receptor and the other as an anion–π receptor. This novel dual role of the 1,2,3-triazolium ring as an anion-binding site has no precedent in the literature.[25]

To probe the efficacy of the anion–π versus hydrogen-bonding interactions to bind anions in solution, the bis(1,2,3-triazolium) receptors $\mathbf{9}^{2+}\cdot 2\mathbf{BF_4}^-$, $\mathbf{10}^{2+}\cdot 2\mathbf{BF_4}^-$, $\mathbf{11}^{2+}\cdot 2\mathbf{BF_4}^-$, and $\mathbf{13}^{2+}\cdot 2\mathbf{BF_4}^-$, end-capped with aromatic or organometallic substituents that have different electronic properties, were prepared. The design of these receptors focused on two 1,2,3-triazolium cations, which could act as recognition motifs by utilizing either hydrogen bonds or their electron-deficient heteroaromatic rings.

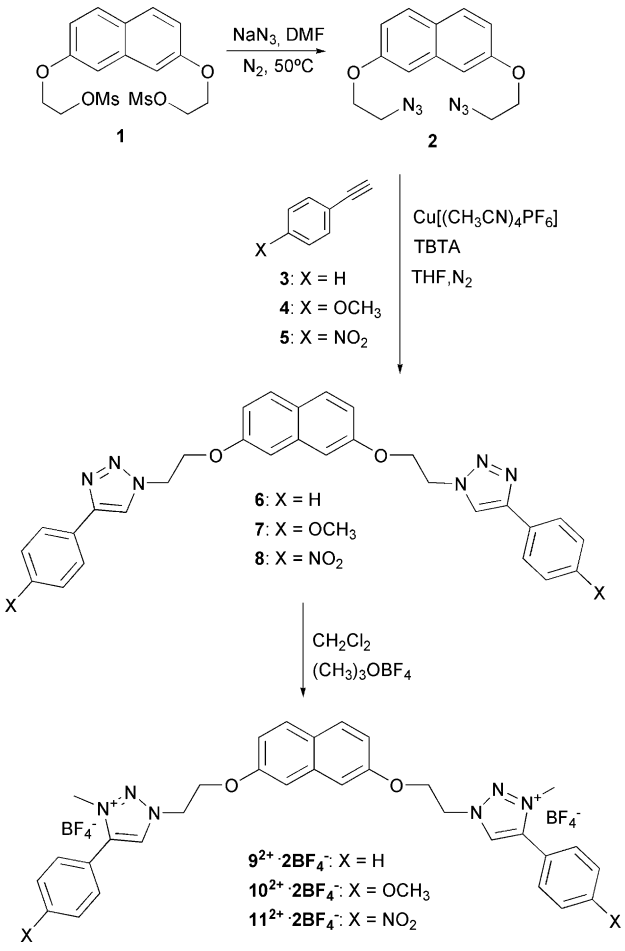

Scheme 1. Synthesis of the receptors $\mathbf{9}^{2+}\cdot 2\mathbf{BF_4}^-$, $\mathbf{10}^{2+}\cdot 2\mathbf{BF_4}^-$, and $\mathbf{11}^{2+}\cdot 2\mathbf{BF_4}^-$.

Results and Discussion

Synthesis

Bidentate triazolium compounds **6**–**8** were prepared by copper(I)-catalyzed azide–alkyne cycloaddition (CuAAC)[26] from 2,7-bis(2-azidoethoxy)naphthalene (**2**), obtained in 87% yield from 2,7-bis(2′-hydroxy-ethoxy)naphthalene bis(methanesulfonate) ester (**1**) and 1-ethynylbenzene (**3**), 1-ethynyl-4-methoxybenzene (**4**), or 1-ethynyl-4-nitrobenzene (**5**), respectively. Subsequent methylation with trimethyloxonium tetrafluoroborate afforded the bis(triazolium) receptors $\mathbf{9}^{2+}\cdot 2\mathbf{BF_4}^-$, $\mathbf{10}^{2+}\cdot 2\mathbf{BF_4}^-$, and $\mathbf{11}^{2+}\cdot 2\mathbf{BF_4}^-$ in moderate yields (33–58%) (Scheme 1).

The bis(triazolium) receptor $\mathbf{13}^{2+}\cdot 2\mathbf{BF_4}^-$ with two end-capping ferrocene moieties was prepared in 58% yield by methylation of bis(triazole) **12** (obtained by coupling the bis(azide) **2** and ethynylferrocene) (Scheme 2).

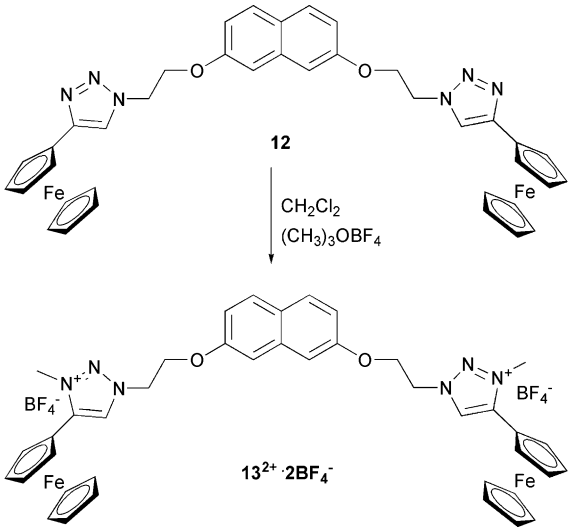

Scheme 2. Synthesis of the receptor $\mathbf{13}^{2+}\cdot 2\mathbf{BF_4}^-$.

Anion-binding studies

NMR studies

The anion-recognition properties of bis(triazolium) receptors $\mathbf{9}^{2+}\cdot 2\mathbf{BF_4}^-$, $\mathbf{10}^{2+}\cdot 2\mathbf{BF_4}^-$, $\mathbf{11}^{2+}\cdot 2\mathbf{BF_4}^-$, and $\mathbf{13}^{2+}\cdot 2\mathbf{BF_4}^-$ were evaluated by ^{1}H NMR spectroscopy in the presence of several anions ($HP_2O_7^{3-}$, $H_2PO_4^-$, SO_4^{2-}, HSO_4^-, NO_3^-, F^-, Cl^-, Br^-, I^-, AcO^-, ClO_4^-, PF_6^-, and $C_6H_5CO_2^-$) added as tetrabutylammonium salts in CD_3CN/CD_3OD (9:1 v/v).

The ^{1}H NMR spectra of receptors $\mathbf{9}^{2+}\cdot 2BF_4^-$, $\mathbf{10}^{2+}\cdot 2BF_4^-$, $\mathbf{11}^{2+}\cdot 2BF_4^-$, and $\mathbf{13}^{2+}\cdot 2BF_4^-$ were very similar and exhibited the following characteristic signals. The first signal set is due to the O–CH_2–CH_2–triazolium environments, which appear as two different triplets at $\delta \approx 5.03$ and 4.57 ppm, and the singlet of the N–CH_3 protons at $\delta = 4.17$ ppm. The second characteristic set of signals correspond to the naphthalene protons: the inner H_d protons of the naphthalene ring appear at $\delta \approx 7.20$ ppm, whereas the outer H_b and H_e protons are located at $\delta = 7.71$ and 7.00 ppm, respectively. The CH_a proton of the triazolium ring is most affected by the electronic nature of the end-capping aromatic group: it appears as a clear, sharp singlet in the range $\delta = 8.55$–8.77 ppm. Additionally, the receptors $\mathbf{9}^{2+}\cdot 2BF_4^-$, $\mathbf{10}^{2+}\cdot 2BF_4^-$, $\mathbf{11}^{2+}\cdot 2BF_4^-$, and $\mathbf{13}^{2+}\cdot 2BF_4^-$ show the expected signals for the end-capping groups.

Thus, addition of the aforementioned set of anions to solutions of the receptors $\mathbf{9}^{2+}\cdot 2BF_4^-$, $\mathbf{10}^{2+}\cdot 2BF_4^-$, $\mathbf{11}^{2+}\cdot 2BF_4^-$, and $\mathbf{13}^{2+}\cdot 2BF_4^-$ in CD_3CN/CD_3OD (9:1 v/v) showed that basic F^- anions promoted deprotonation (see the Supporting Information) and only the addition of $HP_2O_7^{3-}$ and $H_2PO_4^-$ anions induced any remarkable perturbation in the ^{1}H NMR spectra, an early indication of the selectivity of the binding. The observed response depends on the anion added and the electronic character of the aryl substituent of the triazolium ring.

Dihydrogenphosphate anion

Thus, addition of increasing amounts of $H_2PO_4^-$ anions to a solution of $\mathbf{9}^{2+}\cdot 2BF_4^-$, $\mathbf{10}^{2+}\cdot 2BF_4^-$, $\mathbf{11}^{2+}\cdot 2BF_4^-$, and $\mathbf{13}^{2+}\cdot 2BF_4^-$ in CD_3CN/CD_3OD (9:1 v/v) induced similar changes in all the receptors. The most-affected signals were the H_a triazolium protons, which were shifted significantly downfield by $\Delta\delta = 0.51$–0.71 ppm, the inner H_d naphthalene protons, which were shifted (to a lesser degree) downfield by $\Delta\delta = 0.38$–0.42 ppm. On the contrary, the outer H_b and H_e naphthalene protons were shifted upfield by $\Delta\delta = -0.06$ to -0.10 ppm and $\Delta\delta = -0.07$ to -0.12 ppm, respectively. Finally, the triplets corresponding to the O–CH_2–CH_2–triazolium unit were shifted by practically the same magnitude $\Delta\delta = 0.15$ ppm, whereas the N–CH_3 signal was almost unaffected by the presence of the $H_2PO_4^-$ anions. Notably, that during the course of the titrations all the signals were well defined and showed sharp peaks (Figure 1).

Titration of $H_2PO_4^-$ with $\mathbf{9}^{2+}\cdot 2BF_4^-$, $\mathbf{10}^{2+}\cdot 2BF_4^-$, $\mathbf{11}^{2+}\cdot 2BF_4^-$, and $\mathbf{13}^{2+}\cdot 2BF_4^-$ produced considerable changes in the chemical shift of the H_a triazolium protons and inner-cavity H_d naphthyl protons, which demonstrates that these protons are involved in the ligand–anion binding system. The chemical shift of the H_a triazolium proton was monitored by using the WinEQNMR program.[27] Job plot analysis of the titration data provided a 1:2 receptor/anion binding mode and the calculated association constants are given in Table 1.

We hypothesize that K_{11} is related to the electronic distribution around the triazolium cations. We calculated the molecular electrostatic potential (MEP) on the 0.001 electron-density surface of the model compounds **9′**–**11′** and **13′** (Scheme 3). Analysis of the critical points of the MEP shows two maxima (marked in Figure 2 with black circles), one on top of the ring

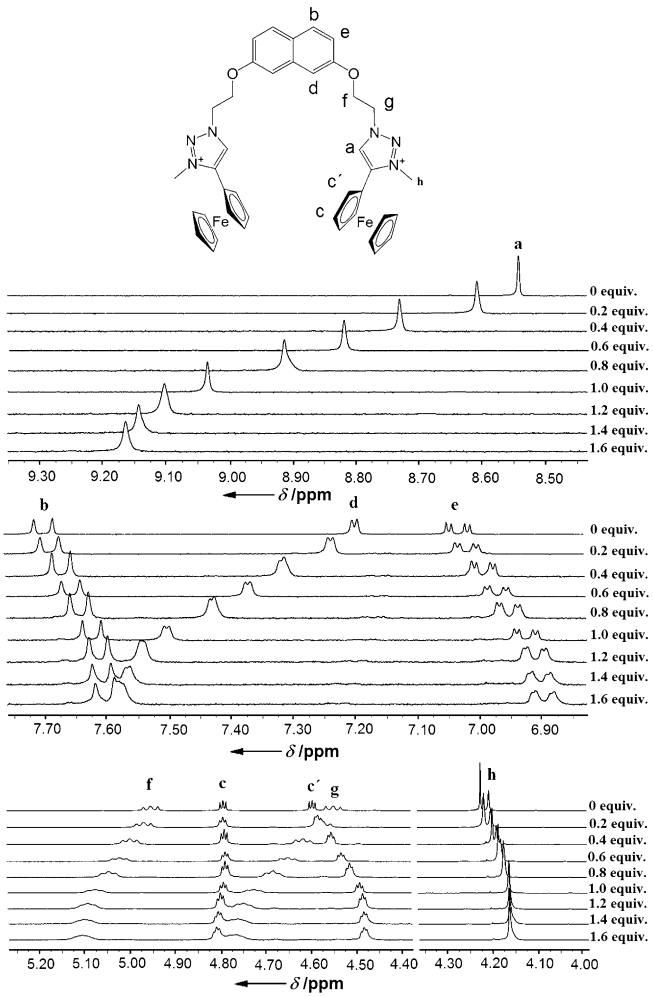

Figure 1. ^{1}H NMR spectral changes observed for the receptor $\mathbf{13}^{2+}\cdot 2BF_4^-$ in CD_3CN/CD_3OD (9:1 v/v) during the addition of $H_2PO_4^-$ ions (up to 1.6 equiv).

Table 1. Association constants for the complexes of receptors $\mathbf{9}^{2+}\cdot 2BF_4^-$, $\mathbf{10}^{2+}\cdot 2BF_4^-$, $\mathbf{11}^{2+}\cdot 2BF_4^-$, and $\mathbf{13}^{2+}\cdot 2BF_4^-$ with the $H_2PO_4^-$ anion and the MEP values of the model compounds **9′**–**11′** and **13′**, respectively.

Complex	K_{11} [M^{-1}][a]	K_{12} [M^{-1}][a]	MEP π	MEP CH
$\mathbf{9}^{2+}\cdot 2H_2PO_4^-$	1592 ± 34	703 ± 50	0.167	0.183
$\mathbf{10}^{2+}\cdot 2H_2PO_4^-$	1107 ± 175	926 ± 89	0.158	0.171
$\mathbf{11}^{2+}\cdot 2H_2PO_4^-$	2961 ± 273	755 ± 63	0.179	0.187
$\mathbf{13}^{2+}\cdot 2H_2PO_4^-$	1772 ± 11	445 ± 31	0.160	0.173

[a] K_{11} is the association constant corresponding to the L+A→LA process; K_{12} is the association constant corresponding to the LA+A→LA_2 process.

(π type), the other on the extension of the C–H_a bond (hydrogen-bonding type).

The positive values (in a.u.) of the MEP in the maxima are given in Table 1. The positive indicated that they are attractive zones for anions (in general, for negative charges). One observation is that, in all cases, the CH part is more attractive than the π part but the increase is small (between 1.04 and 1.10 times greater). This means that it is almost impossible to differentiate between the attractors based on experimental K_{11}

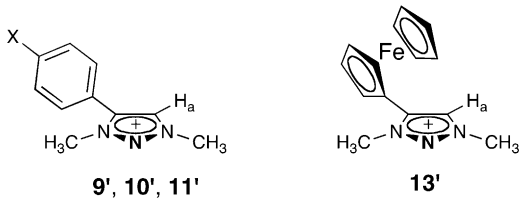

Scheme 3. Model compounds to study the effect of the substituents on the association constants.

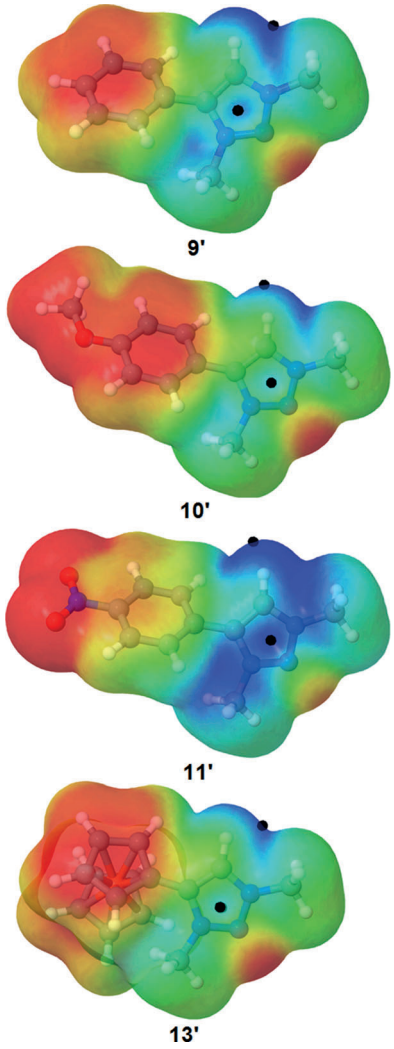

Figure 2. MEPs represented between 0.10 (red) and 0.175 (blue) a.u.

values. The corresponding regression lines are shown in Equations (1) and (2).

$$K_{11} = -(13888 \pm 7508) + (87900 \pm 41888)\text{*MEP CH} \quad (1)$$
$$R^2 = 0.688$$

$$K_{11} = -(10632 \pm 3770) + (75339 \pm 22710)\text{*MEP } \pi \quad (2)$$
$$R^2 = 0.846$$

The correlation is better with the π-type model, but this conclusion is to be handled with care. These combined results, along with the symmetry of the inner signals during the titration process, suggest the formation of a symmetrical complex with an *in–in* conformation in the second step (Figure 3).

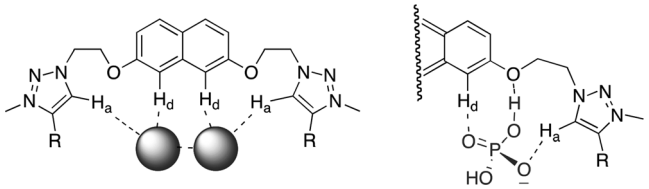

Figure 3. Schematic representation of the binding mode of $H_2PO_4^-$ anions with the receptors.

Hydrogenpyrophosphate trianion

Interestingly, the addition of $HP_2O_7^{3-}$ anions to the receptors $\mathbf{9}^{2+}\cdot\mathbf{2BF_4}^-$, $\mathbf{10}^{2+}\cdot\mathbf{2BF_4}^-$, $\mathbf{11}^{2+}\cdot\mathbf{2BF_4}^-$, and $\mathbf{13}^{2+}\cdot\mathbf{2BF_4}^-$ induced different changes in the ^{1}H NMR spectra of the receptors, especially to the signal of triazolium proton (Figure 4).

Receptors $\mathbf{9}^{2+}\cdot\mathbf{2BF_4}^-$ and $\mathbf{11}^{2+}\cdot\mathbf{2BF_4}^-$ show similar changes to the triazolium H_a proton signal. Thus, addition of $HP_2O_7^{3-}$ (1.5 equiv) to solutions of $\mathbf{9}^{2+}\cdot\mathbf{2BF_4}^-$ and $\mathbf{11}^{2+}\cdot\mathbf{2BF_4}^-$ in CD_3CN/CD_3OD (9:1 v/v) induced splitting of the H_a protons into two different signals. One signal was shifted downfield by $\Delta\delta =$ 0.65 ppm for receptor $\mathbf{9}^{2+}\cdot\mathbf{2BF_4}^-$ (Figure 4a) and $\Delta\delta =$ 0.90 ppm for receptor $\mathbf{11}^{2+}\cdot\mathbf{2BF_4}^-$ (Figure 4b), whereas the other signal was shifted upfield by $\Delta\delta = -0.13$ and -0.25 ppm for $\mathbf{9}^{2+}\cdot\mathbf{2BF_4}^-$ and $\mathbf{11}^{2+}\cdot\mathbf{2BF_4}^-$, respectively (Figure 4a and 4b). Similar behavior was observed during the addition of $HP_2O_7^{3-}$ anions to receptor $\mathbf{13}^{2+}\cdot\mathbf{2BF_4}^-$: a new downfield-shifted peak appears at $\delta = 9.16$ ppm ($\Delta\delta = 0.62$ ppm) and an upfield-shifted peak at $\delta = 7.94$ ppm ($\Delta\delta = -0.60$ ppm) was observed during the titration, which broadened during the addition of the $HP_2O_7^{3-}$ anion (Figure 4d).

The high chemical shifts of the downfield-shifted triazolium protons ($\delta = 9.66$–9.30 ppm) strongly suggest a hydrogen-bonding interaction, whereas the chemical shifts of the upfield-shifted triazolium protons ($\delta = 8.52$–7.94 ppm) appear in the region for neutral triazole protons. At first, the upfield-shifted signals could be assigned to either covalent σ interaction[28] of the triazolium ring with the oxoanion or a direct charge-transfer interaction of the oxoanion with the electron-deficient π-triazolium cation,[29] namely an anion–π interaction. The former is clearly ruled out by comparison of the ^{13}C NMR spectra of the free receptor and the anionic complex, which shows small changes in the chemical shift of the carbon atoms of the triazole ring upon recognition (see later). In all cases, integration of the split signals gives a 1:1 ratio between the downfield-shifted signal, (C–H hydrogen bonding) and the upfield-shifted signal (combined Csp_2–H/anion–π interactions).

From these results, we suggest that hydrogen-bonding and anion–π interactions could occur simultaneously during the recognition event (see below for more details supporting this binding mode).

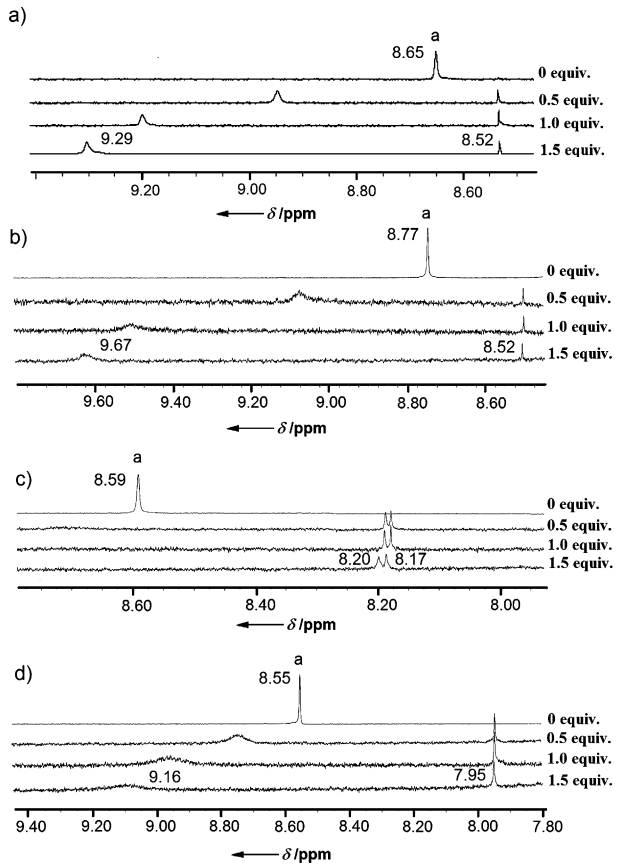

Figure 4. ^{1}H NMR spectral changes observed for the triazolium proton of the receptors a) $\mathbf{9}^{2+}\cdot 2BF_4^-$, b) $\mathbf{11}^{2+}\cdot 2BF_4^-$, c) $\mathbf{10}^{2+}\cdot 2BF_4^-$, and d) $\mathbf{13}^{2+}\cdot 2BF_4^-$ in CD_3CN/CD_3OD (9:1 v/v) during the addition of $HP_2O_7^{3-}$ ions.

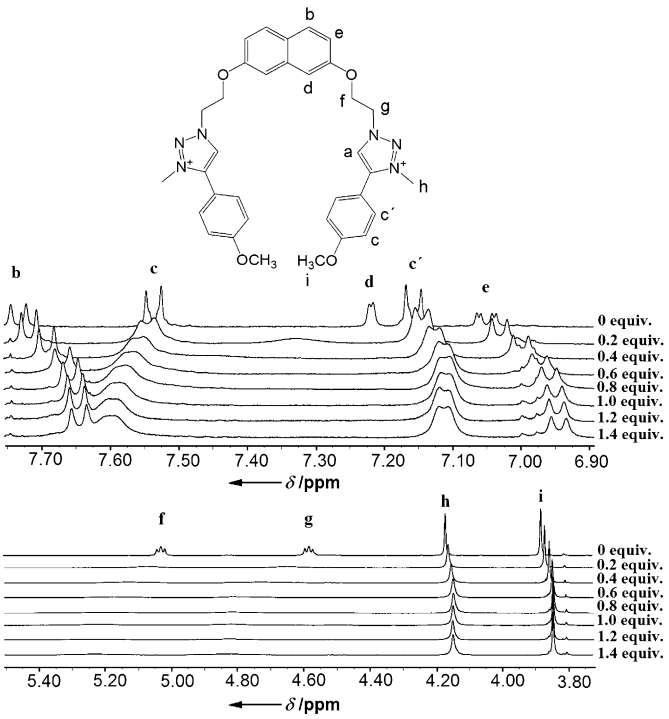

Figure 5. ^{1}H NMR spectral changes of the aromatic (top) and the aliphatic (bottom) regions observed for receptor $\mathbf{10}^{2+}\cdot 2BF_4^-$ in CD_3CN/CD_3OD (9:1 v/v) during the addition of $HP_2O_7^{3-}$ ions (up to 1.4 equiv).

However, the addition of $HP_2O_7^{3-}$ anions to receptor $\mathbf{10}^{2+}\cdot 2BF_4^-$ only promotes the appearance of a new split peak shifted upfield to $\delta = 8.20$ ($\Delta\delta = -0.39$ ppm) and 8.17 ppm ($\Delta\delta = -0.42$ ppm) (Figure 4c). This suggests combined Csp_2–H/anion–π interactions between the heteroaromatic triazolium rings and the bound anion, rather than exclusive hydrogen bonding.[19c,21] In this receptor, the same 1:1 ratio was observed for the two different signals due to the Csp_2–H/anion–π interactions (see the Supporting Information).

On the other hand, addition of $HP_2O_7^{3-}$ anions to solutions of the receptors $\mathbf{9}^{2+}\cdot 2BF_4^-$, $\mathbf{10}^{2+}\cdot 2BF_4^-$, $\mathbf{11}^{2+}\cdot 2BF_4^-$, and $\mathbf{13}^{2+}\cdot 2BF_4^-$ in CD_3CN/CD_3OD (9:1 v/v) promoted similar changes to the rest of the signals in the ^{1}H NMR spectra. The inner naphthalene proton H_d and the methylene protons of the O–CH_2–CH_2–triazolium units got considerably broader and shifted downfield during the titration, which suggested direct participation in the recognition, whereas the outer naphthalene protons were shifted slightly upfield (Figure 5). Variable temperature experiments were also performed but unfortunately no significant changes were observed in the spectra at different temperatures (see the Supporting Information)

Several ^{1}H NMR experiments were performed to clarify the kinetic aspect of the observation of two triazolium proton signals instead of an averaged signal in these bidentate receptors that bear two identical binding arms.

First, after addition of D_2O to a solution of the $\mathbf{9}^{2+}\cdot 2BF_4^-$/pyrophosphate complex in CD_3CN/CD_3OD (9:1 v/v), the spectrum of the free receptor was recovered almost unaltered: only the triazolium protons were shifted downfield ($\Delta\delta = 0.05$ ppm) (see the Supporting Information). One of the most important strategies for pyrophosphate anion recognition utilizes a metal (commonly Zn^{2+}) complex as an anion-binding site. The strong binding affinity between Zn^{2+} and pyrophosphate allows detection of the anion in 100% aqueous solution,[30] therefore, the decomplexation study was also carried out by addition of equimolecular amounts of Zn^{2+}. Thus, after addition of Zn^{2+} to a solution of the $\mathbf{9}^{2+}\cdot 2BF_4^-$/pyrophosphate complex in CD_3CN/CD_3OD (9:1 v/v), the spectrum of the free receptor was recovered and only one triazolium proton signal was present, which clearly indicates the reversibility of the complexation–decomplexation process (see the Supporting Information). Similar behavior was also observed for the $\mathbf{13}^{2+}\cdot 2BF_4^-$/pyrophosphate complex, although addition of substoichiometric amounts of a metal cation induced a progressive upfield shift of the hydrogen-bonded signal, whereas the signal assigned to the anion–π interaction remained unaltered. Further addition of the metal cation led to recovery of the free-receptor spectrum (Figure 6).

However, addition of substoichiometric amounts of metal cation to the $\mathbf{10}^{2+}\cdot 2BF_4^-$/pyrophosphate complex induced partial decomplexation. The resulting spectrum displayed the recovered triazolium signal of the free receptor, together with the two upfield-shifted signals present in the complex. Further addition of the metal cation promoted full recovery of the triazolium proton signal of the free receptor spectrum (see the

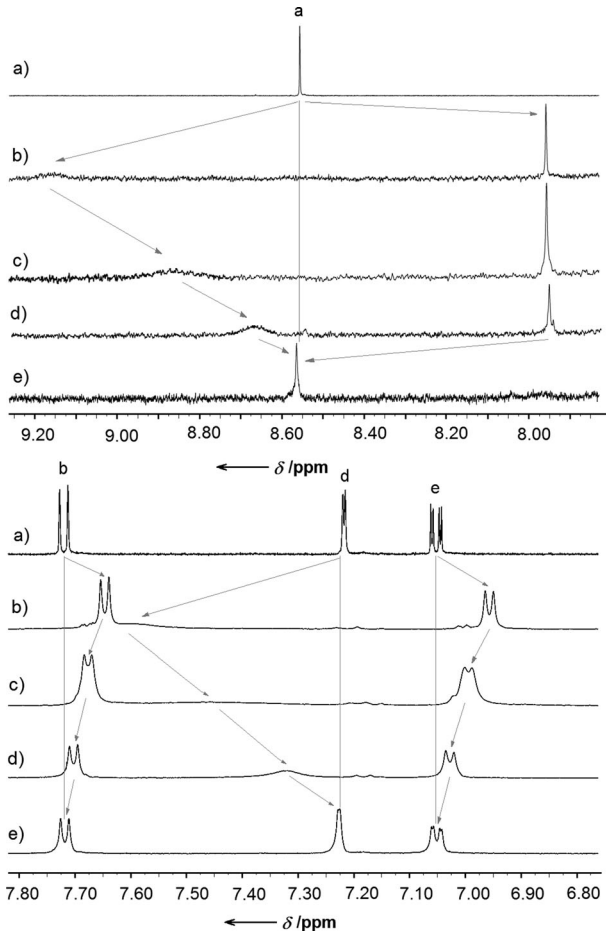

Figure 6. Comparison of two spectral zones of the ^{1}H NMR spectra in CD_3CN/CD_3OD (9:1 v/v) at 20 °C of a) receptor $\mathbf{13^{2+}\cdot 2BF_4^-}$ receptor, b) $\mathbf{13^{2+}\cdot 2BF_4^-}$/pyrophosphate complex, c) $\mathbf{13^{2+}\cdot 2BF_4^-}$/pyrophosphate complex after addition of Zn^{2+} (0.33 equiv) d) $\mathbf{13^{2+}\cdot 2BF_4^-}$/pyrophosphate complex after addition of Zn^{2+} (0.66 equiv), and e) $\mathbf{13^{2+}\cdot 2BF_4^-}$/pyrophosphate complex after addition of Zn^{2+} (1 equiv).

Supporting Information). The combined results of the complexation (Figure 4a, b, and d) and decomplexation events show that the combined C_{aryl}–H/anion–π interaction complexation is faster and its decomplexation slower than the complexation and decomplexation of the complexes with only Csp_2–H hydrogen-bonding interactions.

All these experiments suggest that the complexes do not interconvert directly, and assumes the breaking of three interactions (hydrogen-bonding, anion–π, and C(aryl)–H), plus some conformational changes, but they can interconvert via the free receptor. As the rates involved in this equilibrium are quite different, the averaged signal should not be observed in the NMR spectra.

Finally, in the corresponding 2D NOESY spectrum of the $\mathbf{13^{2+}\cdot 2BF_4^-}$/pyrophosphate complex, cross-peaks between the upfield-shifted triazolium proton and the inner naphthalene protons were observed (completely absent in the free receptor), which provides additional evidence for the spatial proximity of both kinds of proton that enables them to act cooperatively in the recognition process of one end of the pyrophosphate anion by a combination Csp_2–H/anion–π interactions[31] (see the Supporting Information).

These results suggest that although both arms are chemically identical their behavior as oxoanion binding sites is slightly different. In one arm the triazolium ring acts as a hydrogen-bond donor, whereas in the other arm an anion–π interaction reinforced by additional hydrogen bonds with the inner protons of the naphthalene ring takes place. In this context, it has been recently described that in polar media phenyl CH–anion interactions play a greater stabilizing role in oxoanion binding than triazolium $(CH)^+$–anion interactions.[32] These combined effects increase the strength of the binding associated with the upfield-shifted signal and explain why the binding of one end of the oxoanion through combined anion Csp_2–H/anion–π interactions is faster than the binding of the remaining oxoanion end by only hydrogen bonding and, consequently, why the decomplexation is lower than in the system based only on $(CH)^+$–anion interactions.

Next, we investigated why the triazolium protons in the $\mathbf{10^{2+}\cdot 2BF_4^-}$/pyrophosphate complex appeared as two upfield-shifted signals. We believe that these signals probably arise either because after the complexation process both arms adopt slightly different conformations in a slow-exchange situation or as a result of the asymmetric nature of the anion, which gives rise to two different anion π–interactions (see Figure 10c below).

Job plot analysis of the titration data revealed a 1:1 receptor/$HP_2O_7^{3-}$ anion-binding stoichiometry. The calculated association constants were obtained by fitting the titration data to a 1:1 host–guest binding model by using the WinEQNMR program[27] (Table 2).

The calculated association constants showed higher values for the end-capping groups 4-NO_2–C_6H_4 ($4526 \pm 724\ M^{-1}$) and C_6H_5 ($3000 \pm 350\ M^{-1}$) than for 4-CH_3O–C_6H_4 ($1310 \pm 75\ M^{-1}$) and ferrocenyl ($1305 \pm 4\ M^{-1}$). From the calculated values in Table 2, we obtained Equations (3) and (4).

$$K_{11} = -(33348 \pm 7344) + (200317 \pm 40972)\text{*MEP CH} \quad R^2 = 0.923 \tag{3}$$

$$K_{11} = -(23808 \pm 3133) + (158893 \pm 18873)\text{*MEP } \pi \quad R^2 = 0.973 \tag{4}$$

Equation (4) has better correlation than Equation (3), which mirrors the relationship between Equation (2) and Equation (1). Additionally, the slopes for Equations (3) and (4) are a little

Table 2. Association constants for the complexes of receptors $\mathbf{9^{2+}\cdot 2BF_4^-}$, $\mathbf{10^{2+}\cdot 2BF_4^-}$, $\mathbf{11^{2+}\cdot 2BF_4^-}$, and $\mathbf{13^{2+}\cdot 2BF_4^-}$ with the $HP_2O_7^{3<M>}$ anion and the MEP values for the corresponding model compounds.

Complex	K_{11} [M^{-1}]	MEP π	MEP CH	(MEP π+MEP CH)/2
$\mathbf{9^{2+}\cdot HP_2O_7^{3-}}$	3000 ± 350	0.167	0.183	0.175
$\mathbf{10^{2+}\cdot HP_2O_7^{3-}}$	1310 ± 75	0.158	0.171	0.1645
$\mathbf{11^{2+}\cdot HP_2O_7^{3-}}$	4526 ± 724	0.179	0.187	0.183
$\mathbf{13^{2+}\cdot HP_2O_7^{3-}}$	1305 ± 4	0.160	0.173	0.1665

more than double those of Equations (1) and (2), respectively, which indicate that interactions with the $HP_2O_7^{3-}$anion are twice as important as those with the $H_2PO_4^-$ anion. Because $HP_2O_7^{3-}$ interacts with both the π and CH donors, we used the mean of both values (Table 2) to obtain Equation (5).

$$K_{11} = -(28980 \pm 3174) + (182735 \pm 18390) * (\text{MEP CH}{+}\pi)/2$$
$$R^2 = 0.980 \qquad (5)$$

The addition of $HP_2O_7^{3-}$ anions (1 equiv) to receptor $\mathbf{9^{2+}\cdot 2BF_4^-}$ promoted significant changes in the ^{13}C NMR spectrum. Most affected was the N–CH_3 carbon atom, which was shifted upfield by $\Delta\delta = -1.9$ ppm. The C(4) and C(5) carbon atoms of the triazolium ring were also shifted upfield ($\Delta\delta = -0.4$ ppm) with an identical magnitude. The O–CH_2 methylene ($\Delta\delta = +0.5$ ppm), the naphthalene carbon atoms C(1) and C(8) ($\Delta\delta = +0.6$ ppm), and the quaternary carbon atoms C(1a) ($\Delta\delta = +0.4$ ppm) and C(5a) ($\Delta\delta = +0.4$ ppm) were all shifted downfield (Figure 7). The remaining carbon atoms were practically unaffected by the presence of $HP_2O_7^{3-}$ anions.

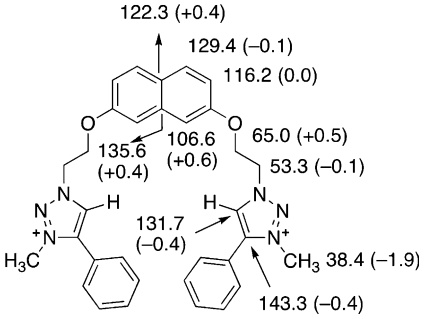

Figure 7. Chemical shifts [ppm] observed in the ^{13}C NMR (CD_3CN/CD_3OD (9:1 v/v) of the receptor $\mathbf{9^{2+}\cdot 2BF_4^-}$ after addition of $HP_2O_7^{3-}$ anions ($\Delta\delta$ values in parentheses).

^{31}P NMR spectral changes were studied after addition of the required receptor (1 equiv) to a solution of the anion in CD_3CN/CD_3OD (9:1 v/v). After addition of $H_2PO_4^-$ (1 equiv) to a solution of the receptor in the same solvent, the ^{31}P NMR signal moves downfield [$\mathbf{10^{2+}\cdot 2BF_4^-}$ (4-CH_3O–C_6H_4; $\Delta\delta = +0.71$ ppm) > $\mathbf{13^{2+}\cdot 2BF_4^-}$ (ferrocenyl; $\Delta\delta = +0.50$ ppm) > $\mathbf{11^{2+}\cdot 2BF_4^-}$ (4-NO_2–C_6H_4; $\Delta\delta = 0.30$ ppm) > $\mathbf{9^{2+}\cdot 2BF_4^-}$ (C_6H_5; $\Delta\delta = +0.1$ ppm)]. The similar values found for the complexes with receptors $\mathbf{10^{2+}\cdot 2BF_4^-}$ and $\mathbf{13^{2+}\cdot 2BF_4^-}$ were expected because of the similar electron-donating abilities of the ferrocenyl and *p*-methoxyphenyl groups.[33]

^{31}P NMR spectral changes were also studied after addition of the receptor (1 equiv) to a solution of $HP_2O_7^{3-}$ in CD_3CN/CD_3OD (9:1 v/v). Protontropy makes both P atoms (P_α and P_β) of the $HP_2O_7^{3-}$ anion isochrones, thus the ^{31}P NMR signal in this solvent appears as a broad singlet (intermediate proton-transfer rate) at $\delta = -6.13$ ppm. After addition of receptor $\mathbf{9^{2+}\cdot 2BF_4^-}$ (1 equiv) in the same solvent, the signal moved upfield to $\delta = -7.28$ ppm ($\Delta\delta = -1.15$ ppm) and became sharper (faster proton transfer). Similar shifts, although with somewhat less extension, were found for the other receptors: $\mathbf{10^{2+}\cdot 2BF_4^-}$ ($\Delta\delta = -0.13$ ppm), $\mathbf{11^{2+}\cdot 2BF_4^-}$ ($\Delta\delta = -0.67$ ppm), and $\mathbf{13^{2+}\cdot 2BF_4^-}$ ($\Delta\delta = -0.03$ ppm).

The reversibility of the complexation–decomplexation process has also been studied by this technique. When a solution of the $\mathbf{9^{2+}\cdot 2BF_4^-}$/pyrophosphate complex in CD_3CN/CD_3OD (9:1 v/v) ($\delta = -7.74$ ppm) was disrupted by addition of D_2O (300 μL) the initial ^{31}P NMR signal for tetrabutylammonium pyrophosphate in the same solvent was almost recovered ($\delta = -8.70$ ppm), which indicated that the anion remains unaltered during the recognition process (see the Supporting Information).

Upfield shifts of $\delta \approx -3.0$ ppm were reported for the hydrogenpyrophosphate trianion with other receptors.[34]

Computational results

The effect of the coordination mode on the triazolium protons

It is important to remember that in 4-substituted triazoles and triazolium cations large downfield shifts of the C–H proton indicate hydrogen bonding of the heteroaromatic ring to the anion,[35] whereas anion–π interactions induce drop in the electron density of the π-deficient triazolium ring and a small upfield shift of the H^{core} proton.[36] Ultimately, the signals appear in the region of the C–H shift for neutral 1,2,3-triazole rings.[37]

We have carried out a computational study on the two model compounds represented in Scheme 4.

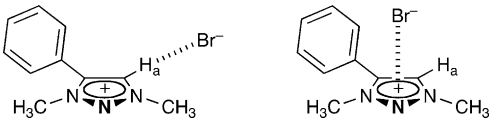

Scheme 4. Model compounds to study the effect of the anion on the triazolium ^1H chemical shift.

The absolute shieldings (σ, ppm) of the triazolium proton H_a calculated by the gauge including atomic orbital (GIAO) method at the B97D/6-31+G(d,p) level, including solvent effects (CH_3CN) by using a polarizable continuum model (PCM) (see the Experimental Section), are as follows: isolated compound ($\sigma = 24.23$ ppm), C–H···Br^- hydrogen-bonding interaction (Scheme 4, left; $\sigma = 22.03$ ppm), and anion–π interaction (Scheme 4, right; $\sigma = 24.36$ ppm). To transform these σ values into chemical shifts (δ, ppm) we calculated the absolute shieldings of 1-methyl-1*H*-1,2,3-triazole and compared them with the experimental ^1H NMR chemical shifts in $[D_6]$DMSO to obtain Equation (6).

$$\delta = (29.1 \pm 2.1) - (0.87 \pm 0.08)\sigma$$
$$n = 3,\ R^2 = 0.992 \qquad (6)$$

This leads to the following δ values: isolated compound ($\delta = 8.08$ ppm), C–H···Br^- hydrogen-bonding interaction ($\delta = 9.98$ ppm), and anion–π interaction ($\delta = 7.96$ ppm). Thus, the

calculated effects ($\Delta\delta = +1.90$ and -0.12 ppm) are in agreement with the qualitative conclusions reported above.

Theoretical modeling

We have calculated the geometries and energies of the neutral receptor $\mathbf{9}^{2+}$ and its complexes with $H_2PO_4^-$, $HP_2O_7^{3-}$, Br^-, and SO_4^{2-} anions at the B97D/6-31+G(d) level including the solvent effect (CH_3CN) by the PCM method (see the Supporting Information).

We obtained three geometries for this receptor (Figure 8), two minima and one structure of imposed C_2 symmetry with a small negative frequency (4 cm^{-1}) with relative energies of 0.0, 2.1, and 22.3 kJ mol^{-1}, respectively.

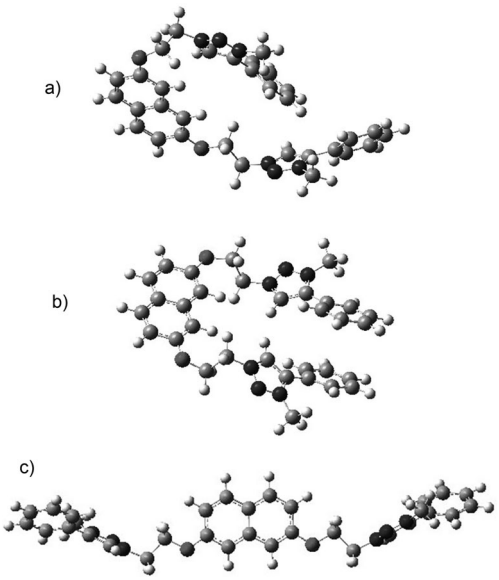

Figure 8. The geometries of neutral receptor $\mathbf{9}^{2+}$. a) Folded minima; b) folded C_2; c) extended conformation, also C_2 symmetry.

For the complex with hydrogenpyrophosphate we obtained two minima, whereas for the complex with the dihydrogenphosphate anion only one minimum was found.

Hydrogenphosphate complex: Starting from the 1:1 complex, only one minimum was located (see the Supporting Information).

The structure corresponds to a H–π interaction with a related interaction energy of -57.3 kJ mol^{-1}. Besides two naphthalene CH units pointing towards an O atom, the OH group points toward the naphthalene ring close to an O–H–π interaction.

A theoretical calculation of the possibility suggested in Figure 3 for the 1:2 complex that leads to the optimized structure represented in Figure 9 gave an interaction energy of -190.1 kJ mol^{-1}.

It is apparent that the stacking involves the naphthalene ring sandwiched between two triazolium cations (Figure 9a), whereas Figure 9b illustrates the hydrogen bonding present in the $H_2PO_4^-$ dimer. Members of our group have already studied

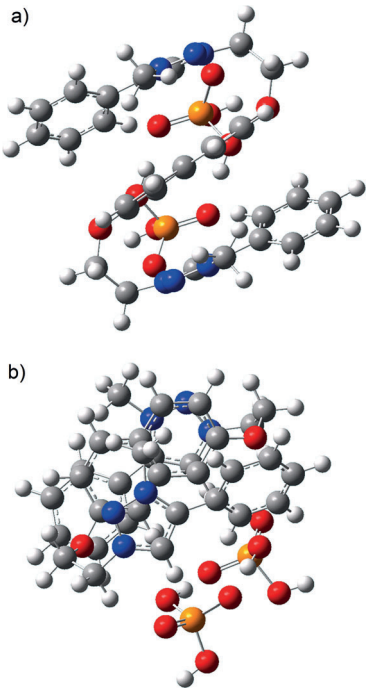

Figure 9. Two views of the optimized structure of the $\mathbf{9}^{2+}\cdot 2H_2PO_4^-$ complex.

the surprising result of hydrogen bonding between two negatively charged molecules, including the hydrogenphosphate anion, to form stable dimers.[38]

Hydrogenpyrophosphate complex: In this case, two minima were located (Figure 10). Both structures are of the H–π class, but show very different participation of the hydrogenpyrophosphate anion: either one half or the whole molecule. However, the interaction energies ($E_i = -97.5$ and -95.9 kJ mol^{-1}) are very similar. A summary of the interaction energies is reported in Table 3.

According to these data, the strongest interaction (the best recognition) takes place with $HP_2O_7^{3-}$; the difference between both kinds of interaction (Figure 10) is very small (1.6 kJ mol^{-1}) and beyond discussion. In all cases, H–π is the sole interaction.

Figure 11 illustrates a comparison of both phosphorus derivatives (values from the calculations carried out in CH_3CN).

The dihydrogenphosphate anion forms a 1:1 complex of type H–π. The receptor is characterized by an experimental K_{11} value of 1592 M^{-1} and a calculated E_i value of -57.3 kJ mol^{-1} with an inter-ring distance (d_π) of 8.2 Å. Then, a second molecule of dihydrogenphosphate enters the receptor, which results in considerable modification of the structure: both anions hydrogen bond with the triazolium ring CH groups, which shortens the binding distance. The association constant K_{12} decreases to 703 M^{-1} but E_i increases to -132.8 kJ mol^{-1}. This disagreement probably arises from the relationship of the experimental results to more dynamic situations in which only one minimum has been calculated.

The hydrogenpyrophosphate trianion behaves similarly, but stops at the 1:1 complex because it is more voluminous and bears three negative charges. The geometry is very similar but both K_{11} and E_i are almost doubled due to electrostatic effects.

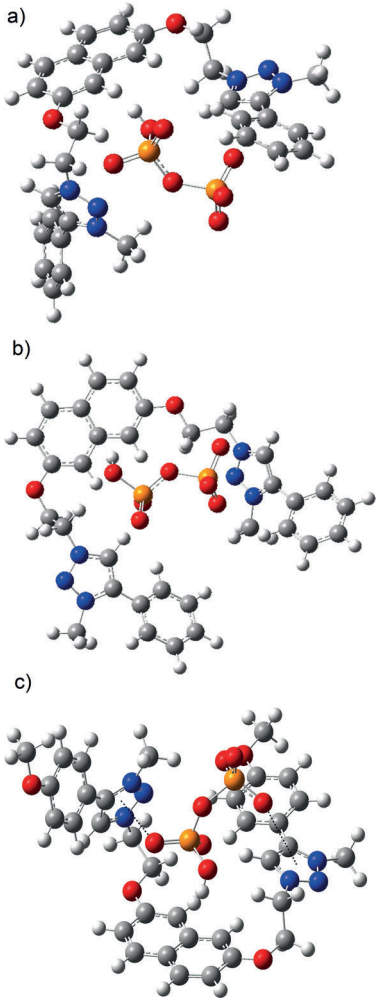

Figure 10. Structure of the $\mathbf{9^{2+}\cdot HP_2O_7^{3-}}$ minima. a) Only one half of the anion is involved in the interactions; b) the whole anion is involved in the interactions. c) Structure of $\mathbf{10^{2+}\cdot HP_2O_7^{3-}}$.

Table 3. Calculated interaction energies (E_i) [kJ mol^{-1}].

Anion	Stoichiometry	Minimum H–π
$H_2PO_4^-$	1:1	−57.3
$H_2PO_4^-$	1:2	−190.1[a]
$HP_2O_7^{3-}$	1:1	−97.5/−95.9

[a] With regards to the free host; with regards to the 1:1 complex, the value is −132.8 kJ mol^{-1}.

Electrochemical studies

The presence of two redox-active ferrocene moieties in the receptor $\mathbf{13^{2+}\cdot 2BF_4^-}$ close to the anion-binding triazolium ring allowed us to perform electrochemical studies to evaluate the electrochemical-sensing properties of $\mathbf{13^{2+}\cdot 2BF_4^-}$. Osteryoung square-wave voltammetry (OSWV) was used to evaluate the anion-binding ability of $\mathbf{13^{2+}\cdot 2BF_4^-}$. In the first instance, a mixture CH_3CN/CH_3OH (9:1 v/v) was used but a strong absorption phenomenon on the electrode surface was observed upon anion addition, whereas utilization of CH_3OH as a solvent inhibited the absorption phenomena. Thus, the electrochemical anion-sensing studies of the bis(triazolium) receptor $\mathbf{13^{2+}\cdot 2BF_4^-}$ were carried out in solution in CH_3OH with $[(n\text{Bu})_4\text{N}]ClO_4$ (0.1 M) as a supporting electrolyte. As expected, receptor $\mathbf{13^{2+}\cdot 2BF_4^-}$ exhibited one peak in the range 0–1.0 V ($E = 0.630$ V) versus Ag/AgCl. Titration studies after addition of $HP_2O_7^{3-}$, $H_2PO_4^-$, SO_4^{2-}, HSO_4^-, NO_3^-, F^-, Cl^-, Br^-, I^-, AcO^-, ClO_4^-, PF_6^-, and $C_6H_5CO_2^-$ anions as their tetrabutylammonium salts to an electrochemical solution of $\mathbf{13^{2+}\cdot 2BF_4^-}$ ($c \sim 10^{-3}$ M in CH_3OH) demonstrated that only the addition of $HP_2O_7^{3-}$ anions promoted a remarkable response by OSWV of this receptor. The addition of $HP_2O_7^{3-}$ revealed a progressive shift of the oxidation peak to a more-negative potential ($E = 0.567$ V; $\Delta E =$ 63 mV) associated with the formation of a complexed species. The current intensity of the peak decreased during the addition of the guest anion (see the Supporting Information). Remarkably, the presence of $H_2PO_4^-$ anions had no effect on OSWV, even when present in large excess. Moreover, when an electrochemical solution of this receptor in CH_3CN was titrated with the strong base $n\text{Bu}_4\text{NOH}$, which definitely leads to deprotonation, a remarkable cathodic shift of the oxidation peak of the receptor was induced ($\Delta E = -409$ mV) after addition of 30 equivalents of base. The magnitude of the oxidation shift is similar to that observed in the case of the F^- anion (see the Supporting Information).

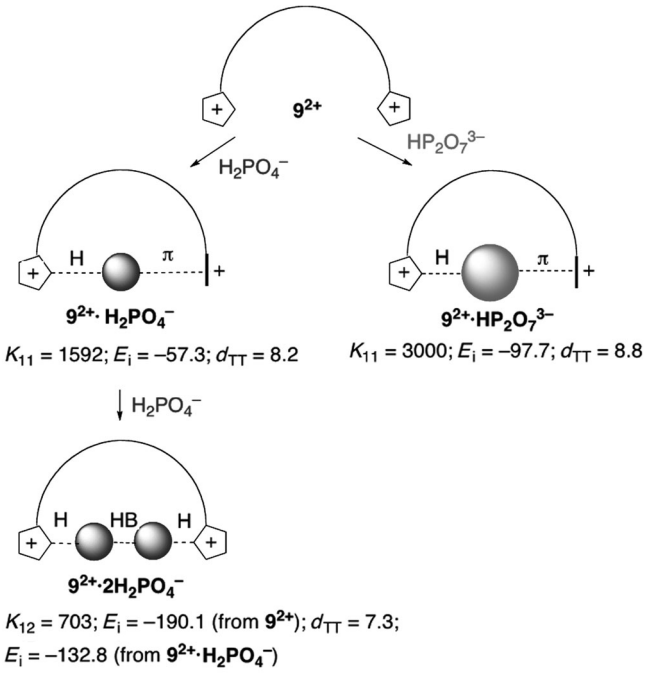

Figure 11. A schematic representation of the behavior of receptor $\mathbf{9^{2+}}$ with the dihydrogenphosphate anion and hydrogenpyrophosphate trianion. d_π is the distance [Å] between the centroids of both triazolium rings.

Conclusion

The synthesis of a new family of bis(triazolium) receptors has been achieved, in which a naphthalene spacer group is decorated with two arms that contain substituted-triazolium-ring

binding sites, end-capped with a ferrocenyl unit or substituted aromatic rings. The prepared receptors have proved to be useful models to explore the potential of a positive interaction between an unprecedented molecular recognition combination of Csp_2–H/anion–π and $(CH)^+$–anion interactions in solution. NMR spectroscopic data indicates that, in some cases, one arm of the triazolium ring acts as a hydrogen-bond donor, whereas the triazolium ring of the second arm behaves as an anion–π receptor, through a combination of Csp_2–H–π and anion–π interactions. The recognition mechanism for oxoanions depends strongly on the electronic nature of the substituents on the aromatic ring and on the characteristic of the anion. Thus, in the case of the hydrogenpyrophosphate trianion the ^{1}H NMR data suggests that hydrogen bonding and anion–π bonding occur simultaneously during the recognition event with $\mathbf{9^{2+}}\cdot\mathbf{2BF_4^-}$($C_6H_5$) and $\mathbf{11^{2+}}\cdot\mathbf{2BF_4^-}$(4-$NO_2$–$C_6H_4$), whereas with electron-rich receptors $\mathbf{10^{2+}}\cdot\mathbf{2BF_4^-}$ (4-OCH_3–C_6H_4) and $\mathbf{13^{2+}}\cdot\mathbf{2BF_4^-}$ (ferrocene) the titration data suggests that only anion–π interactions occur between the heteroaromatic triazolium rings and the bound anion in a half-closed structure. On the other hand, for the dihydrogenphosphate anion the combined results (a downfield shift of the triazolium protons and the symmetry of the inner naphthalene signals during the titration process) suggest the formation of an open hydrogen-bonded symmetrical complex with an *in–in* conformation, which involves combinations of cationic (triazolium) and neutral (naphthalene) C–H hydrogen-bonding interactions and different stoichiometry. We have carried out theoretical calculations at the B97D/6-31+G(d,p) level including solvent effects (PCM model), chemical shift calculations (GIAO), and MEP values. The results were essential for the interpretation of several observations, such as the effect of anions on the ^{1}H NMR chemical shifts of the triazolium protons and the structures of the complexes, particularly those of the phosphorus derivatives. Finally, we were able to relate the electronic structure of the substituted-phenyl (H, $\mathbf{9^{2+}}\cdot\mathbf{2BF_4^-}$; OCH_3, $\mathbf{10^{2+}}\cdot\mathbf{2BF_4^-}$; NO_2, $\mathbf{11^{2+}}\cdot\mathbf{2BF_4^-}$) and the ferrocenyl group ($\mathbf{13^{2+}}\cdot\mathbf{2BF_4^-}$) with the interaction energies, which is a very significant result.[39]

Experimental Section

All reactions were carried out using solvents that were dried by routine procedures. All melting points were determined by means of a Kofler hot-plate melting-point apparatus and are uncorrected. Solution ^{1}H, ^{13}C, and ^{31}P NMR spectra were recorded with a Bruker 200, 300, 400, or 600 MHz spectrometer. The following abbreviations have been used to state the multiplicity of the signals: s (singlet), m (multiplet), and q (quaternary carbon atom). Chemical shifts (δ) in the ^{1}H and ^{13}C NMR spectra are referenced to tetramethylsilane (TMS). Mass spectra were recorded with a Fisons AUTOSPEC 500 VG spectrometer and FAB+ mass spectra were carried out with 3-nitrobenzylalcohol as a matrix. Microanalyses were performed with a Carlo–Erba 1108 instrument. Cyclic voltammetric measurements were performed with a QUICELTRON potentiostat/galvanostat controlled by a personal computer and driven by dedicated software. Cyclic voltammetry was performed with a conventional three-electrode configuration that consisted of platinum working and auxiliary electrodes and a saturated calomel reference electrode. The experiments were carried out in solution ($c \sim 10^{-3}$ M) in the appropriate solvent with [nBu$_4$N][PF$_6$] (0.1 M) as the supporting electrolyte. The solutions were deoxygenated with a stream of N_2 for at least 10 min and the working electrode was cleaned after each run. The cyclic voltammograms were recorded with a scan rate that increased from 0.05 to 1.00 V s^{-1}. The OSWV voltammograms were recorded in the appropriate solvent: The step and the pulse amplitudes were $\Delta Es = 4$ mV; $\Delta Ep = 25$ mV respectively, and the frequency was 15 Hz. Ferrocene was used as an internal reference for the potential calibration and reversibility criteria in all the solvents used.

General procedure for the synthesis of the bis(triazoles) 6, 7, 8, and 12

Tetrakisacetonitrilecopper(I) hexafluorophosphate (0.4 mmol) and tris[(1-benzyl-1*H*-1,2,3-triazol-4-yl)methyl]amine (TBTA) (0.4 mmol) were added to a solution of 2,7-bis(2′-azidoethoxy)naphthalene (1.0 mmol) and 1-ethynylbenzene, 1-ethynyl-4-methylbenzene, or 1-ethynyl-4-nitrobenzene. (3.6 mmol) in dry THF (40 mL). *N*,*N*-Diisopropylethylamine (0.2 mL, 1.15 mmol) was added and the reaction was stirred in the dark for 48 h at rt. The mixture was quenched with a 10% ammonium hydroxide solution (5 mL). The volatile components were removed under vacuum and the precipitated solid was filtered and washed with MeOH (3×50 mL) to give the desired compound.

Compound ***6***: Yield = 90%; m.p. 234 °C (decomposes); ^{1}H NMR (300 MHz, CD_3CN/CD_3OD 9:1): $\delta = 8.24$ (s, 2H), 7.81 (d, $J = 9$ Hz, 4H), 7.66 (d, $J = 9$ Hz, 2H), 7.40 (d, $J = 9$ Hz, 4H), 7.32 (d, $J = 9$ Hz, 2H), 7.12 (d, $J = 2.3$ Hz, 2H), 7.96 (dd, $J = 9$, 2.3 Hz, 2H), 4.81 (t, $J = 5$ Hz, 4H), 4.50 ppm (t, $J = 5$ Hz, 4H); ^{13}C NMR (50 MHz, [D$_6$]acetone): $\delta = 156.7$, 146.7, 135.8, 131.1, 129.6, 129.3, 128.2, 125.5, 124.6, 122.4, 116.4, 106.4, 106.9, 66.46, 49.65 ppm; MS (ESI): *m/z* calcd for $C_{30}H_{26}N_6O_2$: 502.5 $[M+1]^+$; found: 503.5.

Compound ***7***: Yield = 85%; m.p. 248 °C (decomposes); ^{1}H NMR (200 MHz, CD_3CN/CD_3OD 9:1): $\delta = 8.14$ (s, 2H), 7.72 (d, $J = 9.0$ Hz, 4H), 7.65 (d, $J = 8.9$ Hz, 2H), 7.20 (d, $J = 2.3$ Hz, 2H), 6.96 (m, 6H), 4.79 (t, $J = 5$ Hz, 4H), 4.49 (t, $J = 5$ Hz, 4H), 3.78 ppm (s, 6H); ^{13}C NMR (50 MHz, [D$_6$]DMSO): $\delta = 160.3$, 157.7, 147.6, 136.8, 130.5, 127.8, 125.5, 124.6, 122.3, 117.4, 115.6, 107.9, 67.4, 56.5, 50.5 ppm; MS (ESI): *m/z* calcd for $C_{32}H_{30}N_6O_4$: 563.23 $[M+H]^+$; found: 563.23.

Compound ***8***: Yield = 75%; m.p. 212 °C (decomposes); ^{1}H NMR (300 MHz, CD_3CN/CD_3OD 9:1): $\delta = 8.43$ (s, 2H), 8.25 (d, $J = 9$ Hz, 4H), 8.03 (d, $J = 9$ Hz, 4H), 7.65 (d, $J = 9$ Hz, 2H), 7.13 (d, $J = 2$ Hz, 2H), 6.96 (dd, $J = 2$, 8.9 Hz, 2H), 4.85 (t, $J = 5$ Hz, 4H), 4.51 ppm (t, $J = 5$ Hz, 4H); ^{13}C NMR (75 MHz, [D$_6$]DMSO): $\delta = 156.7$, 147, 144.9, 137.6, 135.8, 129.6, 129.2, 128.2, 126.4, 124.9, 116.5, 107, 66.3, 49.9 ppm; MS (ESI): *m/z* calcd for $C_{30}H_{24}N_8O_6$: 592.18 $[M+H]^+$; found: 592.18.

Compound ***12***: Yield = 56%; m.p. 211 °C (decomposes); ^{1}H NMR (300 MHz, CD_3CN/CD_3OD 9:1): $\delta = 7.92$ (s, 2H), 7.65 (d, $J = 9$ Hz, 2H), 7.12 (d, $J = 2$ Hz, 2H) 6.96 (dd, $J = 9$, 2 Hz, 2H), 4.76 (t, $J = 4.8$ Hz, 4H), 4.67 (t, $J = 2$ Hz, 4H), 4.48 (t, $J = 4.8$ Hz, 4H), 4.25 (t, $J = 2$ Hz, 4H), 3.95 ppm (s, 10H); ^{13}C NMR (75 MHz, [D$_6$]DMSO): $\delta = 206.5$, 156.4, 145.2, 129.15, 121.2, 115.9, 107, 75.97, 69.2, 68.2, 66.3, 66.2, 64.9, 49.0, 30.65, 15.1 ppm; MS (ESI): *m/z* calcd for $C_{38}H_{34}Fe_2N_6$: 718.15 $[M+H]^+$; found: 718.15.

General procedure for the synthesis of the bis(triazolium) receptors $\mathbf{9^{2+}}\cdot\mathbf{2BF_4^-}$, $\mathbf{10^{2+}}\cdot\mathbf{2BF_4^-}$, $\mathbf{11^{2+}}\cdot\mathbf{2BF_4^-}$, and $\mathbf{13^{2+}}\cdot\mathbf{2BF_4^-}$

A suspension of bis(triazole) **6**, **7**, **8**, or **12** (0.79 mmol) in dry dichloromethane (20 mL) was treated with trimethyloxonium tetra-

fluoroborate (1.60 mmol) and the reaction mixture was stirred under N_2 for 48 h at rt. Methanol (2 mL) was added and the volatile components were removed under vacuum. The resulting residue was purified by silica gel column chromatography ($CHCl_3$/CH_2OH 9:1) to give the desired compound.

Receptor $\mathbf{9^{2+}\cdot 2BF_4^-}$: Yield = 40%; m.p. 290 °C (decomposes); ^{1}H NMR (400 MHz, CD_3CN/CD_3OD 9:1): δ = 8.65 (s, 2H), 7.71 (d, J = 8 Hz, 2H), 7.45–7.30 (m, 10H), 7.20 (d, J = 6 Hz, 2H), 7.02 (dd, J = 9, 3 Hz, 2H), 5.03 (t, J = 5 Hz, 4H), 4.57 (t, J = 5 Hz, 4H), 4.17 ppm (s, 6H); ^{13}C NMR (75 MHz, [D$_4$]CD_3OD): δ = 156.4, 143.3, 135.6, 131.7, 129.4, 129.3, 129.1, 124.9, 122.3, 116.2, 106.6, 65.0, 53.3, 38.4 ppm; MS (ESI): *m/z* calcd for $C_{32}H_{32}BF_4N_6O_2$: 619.26 $[M^{2+}+BF_4^-]^+$; found: 619.26.

Receptor $\mathbf{10^{2+}\cdot 2BF_4^-}$: Yield = 33%; m.p. 195 °C (decomposes); ^{1}H NMR (400 MHz, CD_3CN/CD_3OD 9:1): δ = 8.59 (s, 2H), 7.73 (d, J = 8 Hz, 2H), 7.53 (d, J = 12 Hz, 4H), 7.22 (d, J = 4 Hz, 2H), 7.15 (d, J = 12 Hz, 4H), 7.04 (dd, J = 8, 4 Hz, 2H), 5.03 (t, J = 4 Hz, 4H), 4.58 (t, J = 4 Hz, 4H), 4.17 (s, 6H), 3.88 ppm (s, 6H); ^{13}C NMR (100 MHz, [D$_6$]acetone): δ = 162.2, 156.5, 143.4, 135.8, 131.0, 129.2, 128.8, 125.0, 116.3, 114.8, 114.5, 106.7, 65.1, 55.0, 53.4, 38.3 ppm; MS (ESI): *m/z* calcd for $C_{34}H_{36}B_2F_8N_6O_4$: 679.28 $[M^{2+}+BF_4^-]^+$; found: 679.28.

Receptor $\mathbf{11^{2+}\cdot 2BF_4^-}$: Yield = 30%; m.p. 230 °C (decomposes); ^{1}H NMR (400 MHz, CD_3CN/CD_3OD 9:1): δ = 8.76 (s, 2H), 8.41 (d, J = 12 Hz, 4H), 7.82 (d, J = 12 Hz, 4H), 7.72 (d, J = 8 Hz, 2H), 7.21 (d, J = 4 Hz, 2H), 7.04 (dd, J = 8, 4 Hz, 2H), 5.07 (t, J = 4 Hz, 4H), 4.57 (t, J = 4 Hz, 4H), 4.19 ppm (s, 6H); ^{13}C NMR (100 MHz, [D$_6$]acetone): δ = 206.9, 156.5, 149.5, 141.1, 135.7, 131.6, 130.9, 129.8, 129.5, 129.2, 124.7, 116.6, 107.2, 65.3, 53.6, 31.1 ppm; MS (ESI): *m/z* calcd for $C_{32}H_{30}B_2F_8N_8O_6$: 706.23 $[M^{2+}+BF_4^-]^+$; found: 706.23.

Receptor $\mathbf{13^{2+}\cdot 2BF_4^-}$: Yield = 58%; m.p. 136 °C (decomposes); ^{1}H NMR (400 MHz, CD_3CN/CD_3OD 9:1): δ = 8.54 (s, 2H), 7.70 (d, J = 8 Hz, 2H), 7.19 (d, J = 4 Hz, 2H), 7.03 (dd, J = 8, 4 Hz, 2H), 4.95 (t, J = 5 Hz, 4H), 4.79 (t, J = 2 Hz, 4H,), 4.59 (t, J = 5 Hz, 4H), 4.55 (t, J = 2 Hz, 4H), 4.23 (s, 6H), 4.21 ppm (s, 6H); ^{13}C NMR (100 MHz, [D$_6$]acetone): δ = 156, 144.5, 136.2, 129.7, 128.5, 125.4, 116.7, 107.2, 71.6, 70.6, 69.4, 65.6, 53.7, 39.2 ppm; MS (ESI): *m/z* calcd for $C_{40}H_{40}B_2F_8Fe_2N_6O_2$: 835.19 $[M^{2+}+BF_4^-]^+$; found: 835.19.

Computational details

The geometries of the systems were optimized at the B97D/6-31+G(d,p) level[40] taking into account the effect of the solvent (CH_3CN) by means of the PCM method.[41] The calculations were carried out with the Gaussian 09 program.[42] The absolute chemical shielding was calculated with the GIAO method[43] at the same computational level as the geometry optimization. The molecular electrostatic potential[44] of the model compounds was evaluated with the Gaussian 09 facilities, analyzed on the 0.001 au electron-density isosurface with the wave-function analysis surface-analysis suite (WFA-SAS) program,[45] and represented with the Jmol package.[46]

Acknowledgements

This work was supported by the European Commission FP7-PEOPLE-2012-CIG No. 321716 and Ministerio de Ciencia e Innovación of Spain and FEDER, projects CTQ2011-27175 and CTQ2013-46096-P, Fundación Séneca (CARM) Project (18948/JLI/13). Thanks are also given to the Ministerio de Economía y Competitividad of Spain (Project CTQ2012-13129-C02-02) and the Comunidad Autónoma de Madrid (Project MADRISOLAR2, ref. S2009/PPQ-1533). F.Z. acknowledges the Ministerio de Economía y Competitividad of Spain for a contract of the Subprogram Juan de la Cierva, 2012. A.C. acknowledges the Ministerio de Ciencia e Innovación of Spain for funding his work by a Ramón y Cajal Program contract.

Keywords: anions · chemosensors · density functional calculations · noncovalent interactions · recognition

[1] For general references about anion recognition see: a) A. Bianchi, K. Bowman-James, E. García-España, *Supramolecular Chemistry of Anions*, Wiley-VCH, New York, **1997**; b) J. L. Sessler, P. A. Gale, W.-S. Cho, *Anion Receptor Chemistry*, RSC Publishing, The Royal Society of Chemistry, Cambridge, **2006**; c) R. Vilar, *Structure and Bonding, Vol. 129: Recognition of Anions*, Springer, Berlin Heidelberg, **2008**; P. A. Gale, N. Busschaert, C. J. E. Haynes, L. E. Karagiannidis, I. L. Kirby, *Chem. Soc. Rev.* **2014**, *43*, 205–241.

[2] B. Schulze, U. S. Schubert, *Chem. Soc. Rev.* **2014**, *43*, 2522–2571.

[3] Y. Li, A. H. Flood, *J. Am. Chem. Soc.* **2008**, *130*, 12111–12122.

[4] H. C. Kolb, K. B. Sharpless, *Drug Discovery Today* **2003**, *8*, 1128–1137.

[5] Y. Bourne, H. C. Kolb, Z. Radic, K. B. Sharpless, P. Taylor, P. Marchot, *Proc. Natl. Acad. Sci. USA* **2004**, *101*, 1449–1454.

[6] A. Brik, J. Alexandratos, Y. C. Lin, J. H. Elder, A. J. Olson, A. Wlodawer, D. S. Goodsell, C. H. Wong, *ChemBioChem* **2005**, *6*, 1167–1169.

[7] J. K. Pokorski, L. M. M. Jenkins, H. Q. Feng, S. R. Durell, Y. W. Bai, D. H. Appella, *Org. Lett.* **2007**, *9*, 2381–2383.

[8] A. Frontera, *Coord. Chem. Rev.* **2013**, *257*, 1716–1727.

[9] A. Kumar, P. S. Pandey, *Org. Lett.* **2008**, *10*, 165–168.

[10] R. K. Chhatra, A. Kumar, P. S. Pandey, *J. Org. Chem.* **2011**, *76*, 9086–9089.

[11] J. J. Fiol, M. Barceló-Oliver, A. Tasada, A. Frontera, A. Terrón, A. García-Raso, *Coord. Chem. Rev.* **2013**, *257*, 2705–2715.

[12] B. Schulze, C. Friebe, M. D. Hager, W. Günther, U. Köhn, B. O. Jahn, H. Görls, U. S. Schubert, *Org. Lett.* **2010**, *12*, 2710–2713.

[13] N. G. White, P. D. Beer, *Org. Biomol. Chem.* **2013**, *11*, 1326–1333.

[14] T. Romero, A. Caballero, A. Tarraga, P. Molina, *Org. Lett.* **2009**, *11*, 3466–3419.

[15] N. G. White, S. Carvalho, V. Felix, P. D. Beer, *Org. Biomol. Chem.* **2012**, *10*, 6951–6959.

[16] L. C. Gilday, N. G. White, P. D. Beer, *Dalton Trans.* **2012**, *41*, 7092–7097.

[17] a) D. Quiñonero, C. Garau, C. Rotger, A. Frontera, P. Ballester, A. Costa, P. M. Deyá, *Angew. Chem. Int. Ed.* **2002**, *41*, 3389–3392; *Angew. Chem.* **2002**, *114*, 3539–3542; b) I. Alkorta, J. Elguero, *J. Am. Chem. Soc.* **2002**, *124*, 8593–8598; c) M. Mascal, *Angew. Chem. Int. Ed.* **2006**, *45*, 2890–2893; *Angew. Chem.* **2006**, *118*, 2956–2959; d) M. Mascal, I. Yakovlev, E. B. Nikitin, J. C. Fettinger, *Angew. Chem. Int. Ed.* **2007**, *46*, 8782–8784; *Angew. Chem.* **2007**, *119*, 8938–8940; e) B. L. Schottel, H. T. Chifotides, K. R. Dunbar, *Chem. Soc. Rev.* **2008**, *37*, 68–83;f) O. B. Berryman, D. W. Johnson, *Chem. Commun.* **2009**, 3143–3153.

[18] a) R. P. Matthews, T. Welton, P. A. Hunt, *Phys. Chem. Chem. Phys.* **2014**, *16*, 3238–3253; b) S. E. Wheeler, *Acc. Chem. Res.* **2013**, *46*, 1029–1038.

[19] a) S. Guha, S. Saha, *J. Am. Chem. Soc.* **2010**, *132*, 17674–17677; b) O. B. Berryman, A. C. Sather, B. P. Hay, J. S. Meisner, D. W. Johnson, *J. Am. Chem. Soc.* **2008**, *130*, 10895–10897; c) G. Gil-Ramírez, E. C. Escudero-Adan, J. Benet-Buchholz, P. Ballester, *Angew. Chem. Int. Ed.* **2008**, *47*, 4114–4118; *Angew. Chem.* **2008**, *120*, 4182–4186; d) H. T. Chifotides, B. L. Schottel, K. R. Dunbar, *Angew. Chem. Int. Ed.* **2010**, *49*, 7202–7207; *Angew. Chem.* **2010**, *122*, 7360–7365; e) Y. S. Rosokha, S. V. Lindeman, S. V. Rosokha, J. K. Kochi, *Angew. Chem. Int. Ed.* **2004**, *43*, 4650–4652; *Angew. Chem.* **2004**, *116*, 4750–4752.

[20] P. Ballester, *Acc. Chem. Res.* **2013**, *46*, 874–884.

[21] K.-C. Chang, T. Minami, P. Koutnik, P. Y. Savechenkov, Y. Liu, P. Anzanbacher Jr., *J. Am. Chem. Soc.* **2014**, *136*, 1520–1525.

[22] N. L. Kilah, M. D. Wise, C. J. Serpell, A. L. Thompson, N. G. White, K. E. Christensen, P. D. Beer, *J. Am. Chem. Soc.* **2010**, *132*, 11893–11895.

[23] M. G. Chudzinski, C. A. McClary, M. S. Taylor, *J. Am. Chem. Soc.* **2011**, *133*, 10559–10567.

[24] G. T. Spence, C. J. Serpell, J. Sardinha, P. J. Costa, V. Félix, P. D. Beer, *Chem. Eur. J.* **2011**, *17*, 12955–12966.

[25] J. M. Aizpurua, R. M. Fratila, Z. Monasterio, N Perez-Esnaola, E. Andreieff, A. Irastorza, M. Sagartzazu-Aizpurua, *New J. Chem.* **2014**, *38*, 474 – 480.
[26] J. E. Hein, J. C. Tripp, L. B. Krasnova, K. B. Sharpless, V. V. Fokin, *Angew. Chem. Int. Ed.* **2009**, *48*, 8018 – 8021; *Angew. Chem.* **2009**, *121*, 8162 – 8165.
[27] M. J. Hynes, *J. Chem. Soc. Dalton Trans.* **1993**, 311 – 312.
[28] B. J. Hay, V. S. Bryantsev, *Chem. Commun.* **2008**, 2417 – 2428.
[29] C. Caumes, O. Roy, S. Faure, C. Taillefumier, *J. Am. Chem. Soc.* **2012**, *134*, 9553 – 9556.
[30] S. K. Kim, D. H. Lee, J-I. Hong, J. Yoon, *Acc. Chem. Res.* **2009**, *42*, 23 – 31.
[31] V. Lloveras, A. Caballero, A. Tarraga, M. D. Velasco, A. Espinosa, K. Wurst, D. J. Evans, J. Vidal-Gancedo, C. Rovira, P. Molina, J. Veciana, *Eur. J. Inorg. Chem.* **2005**, 2436 – 2450.
[32] J. Cai, B. J. Hay, N. J. Young, X. Yang, J. L. Sessler, *Chem. Sci.* **2013**, *4*, 1560 – 1567.
[33] J. Cai, J. L. Sessler, *Chem. Soc. Rev.* **2014**, *43*, 6198 – 6213.
[34] K. Ghosh, A. R. Sarkar, A. Samadder, A. R. Khuda-Bukhsh, *Org. Lett.* **2012**, *14*, 4314 – 4317.
[35] a) Q.-Y. Cao, T. Pradhan, S. Kim, J. S. Kim, *Org. Lett.* **2011**, *13*, 4386 – 4389; b) N. G. White, A. R. Colaco, I. Marques, V. Felix, P. D. Beer, *Org. Biomol. Chem.* **2014**, *12*, 4924 – 4931.
[36] M. M. Watt, L. N. Zakharov, M. H. Haley, D. W. Johnson, *Angew. Chem. Int. Ed.* **2013**, *52*, 10275 – 10280; *Angew. Chem.* **2013**, *125*, 10465 – 10470.
[37] a) For a preliminary communication see: A. Caballero, F. Zapata, L. Gonzalez, P. Molina, I. Alkorta, J. Elguero, *Chem. Commun.* **2014**, *50*, 4680 – 4682; b) F. Zapata, A. Caballero, P. Molina, I. Alkorta, J. Elguero, *J. Org. Chem.* **2014**, *79*, 6959 – 6969.
[38] a) I. Mata, I. Alkorta, E. Molins, E. Espinosa, *ChemPhysChem* **2012**, *13*, 1421 – 1424; b) I. Mata, I. Alkorta, E. Molins, E. Espinosa, *Chem. Phys. Lett.* **2013**, *555*, 106 – 109.
[39] V. Nikolova, S. Ilieva, B. Galabov, H. F. Schaeffer, *J. Org. Chem.* **2014**, *79*, 6823 – 6831.
[40] S. Grimme, *J. Comput. Chem.* **2006**, *27*, 1787 – 1799.
[41] a) S. Miertuš, E. Scrocco, J. Tomasi, *Chem. Phys.* **1981**, *55*, 117 – 129; b) J. Tomasi, M. Persico, *Chem. Rev.* **1994**, *94*, 2027 – 2094; c) B. Mennucci, R. Cammi, *Continuum Solvation Models in Chemical Physics. From Theory to Application*, Wiley, Chichester, **2007**.
[42] Gaussian 09, Revision A.1, M. J. Frisch, G. W. Trucks, H. B. Schlegel, G. E. Scuseria, M. A. Robb, J. R. Cheeseman, G. Scalmani, V. Barone, B. Mennucci, G. A. Petersson, H. Nakatsuji, M. Caricato, X. Li, H. P. Hratchian, A. F. Izmaylov, J. Bloino, G. Zheng, J. L. Sonnenberg, M. Hada, M. Ehara, K. Toyota, R. Fukuda, J. Hasegawa, M. Ishida, T. Nakajima, Y. Honda, O. Kitao, H. Nakai, T. Vreven, J. A. Montgomery, Jr., J. E. Peralta, F. Ogliaro, M. Bearpark, J. J. Heyd, E. Brothers, K. N. Kudin, V. N. Staroverov, R. Kobayashi, J. Normand, K. Raghavachari, A. Rendell, J. C. Burant, S. S. Iyengar, J. Tomasi, M. Cossi, N. Rega, J. M. Millam, M. Klene, J. E. Knox, J. B. Cross, V. Bakken, C. Adamo, J. Jaramillo, R. Gomperts, R. E. Stratmann, O. Yazyev, A. J. Austin, R. Cammi, C. Pomelli, J. W. Ochterski, R. L. Martin, K. Morokuma, V. G. Zakrzewski, G. A. Voth, P. Salvador, J. J. Dannenberg, S. Dapprich, A. D. Daniels, Ö. Farkas, J. B. Foresman, J. V. Ortiz, J. Cioslowski, D. J. Fox, Gaussian, Inc., Wallingford CT, **2009**.
[43] a) F. London, *J. Phys. Radium* **1937**, *8*, 397 – 409; b) R. Ditchfield, *Mol. Phys.* **1974**, *27*, 789 – 807.
[44] E. Scrocco, J. Tomasi in *Topics in Current Chemistry, Vol. 42: New Concepts II* (Eds.: A. Davison, M. J. S.Dewar), Springer, Berlin Heidelberg, **1973**, pp. 95 – 70.
[45] F. Bulat, A. Toro-Labbé, T. Brinck, J. Murray, P. Politzer, *J. Mol. Model.* **2010**, *16*, 1679 – 1691.
[46] Jmol:, an open-source Java viewer for chemical structures in 3D, version 13.0. http://www.jmol.org/, accessed on September 26th, **2013**.

Received: January 19, 2015
Published online on ■■ ■■, 0000

FULL PAPER

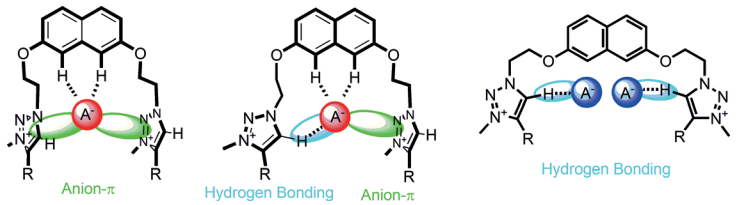

Teamwork! Evidence of combined non-covalent interactions in the recognition process of oxoanions by bis(triazolium) receptors is reported (see figure).

Anion Recognition

F. Zapata, L. Gonzalez, A. Caballero, I. Alkorta,* J. Elguero, P. Molina**

■■ – ■■

Dual Role of the 1,2,3-Triazolium Ring as a Hydrogen-Bond Donor and Anion–π Receptor in Anion-Recognition Processes